DNA Nanotechnology

DOI: 10.1002/ange.201207914

# Non-covalent Single Transcription Factor Encapsulation Inside a DNA Cage**

*Robert Crawford, Christoph M. Erben, Javier Periz, Lucy M. Hall, Tom Brown, Andrew J. Turberfield, and Achillefs N. Kapanidis**

Regulation of gene expression is fundamental for cell development, maintenance, and growth. Gene regulation occurs mainly at the level of transcription, controlled primarily by DNA-binding proteins known as transcription factors (TFs). For example, the delivery of just four TFs to fully differentiated cells can cause them to revert to a stem-cell-like state, offering promise for regenerative medicine.[1] The ability to influence gene regulation by tuning intracellular TF levels would constitute a powerful method for the study of regulation pathways or the development of therapeutic applications.[2]

An elegant approach to the control of gene expression is to reversibly encapsulate the TFs in a drug-delivery cage. Within the cage, the TF cannot bind cellular DNA and is inactive; the cage can then be opened using external triggers, releasing and thus activating the TF. Molecular cages designed for encapsulation vary in size and fabrication method: fullerenes (approximately 1 nm) can encapsulate single atoms;[3] hollow metal nanoparticles[4] (approximately 100 nm) for proteins; and liposomes (100–800 nm) for drugs[5] or fluorescent molecules.[6] TF encapsulation by supramolecular nanoparticles (approximately 50 nm) for intracellular delivery has recently been reported.[7]

Herein, we report a novel cage for a TF constructed using DNA. A DNA cage offers many advantages: for example, cages of dimensions similar to protein targets can be designed rationally to self-assemble in a single, rapid, and facile step. Examples of such DNA nanostructures range from polyhedra,[8] to much larger structures based on DNA origami.[9] DNA cages can be reconfigured, with edges extended or broken in the presence of specific oligonucleotides.[10] DNA can be site-specifically modified with chemical groups, fluorophores, or targeting peptides[2,11] to monitor the cage–protein interactions, subcellular localization, or specific cell targeting; covalent linkers have been used to encapsulate proteins inside a DNA cage.[12] DNA cages have been successfully internalized into mammalian cells[13] and have exhibited enhanced resistance to enzymatic digestion,[14] when compared with linear dsDNA. In vivo cloning techniques for amplifying DNA nanostructures may also substantially reduce the fabrication costs of DNA cages.[15]

In this work, we present a DNA cage for the TF catabolite activator protein (CAP), a global regulator of more than 100 genes.[16] In the presence of its allosteric effector, cyclic adenosine monophosphate (cAMP), CAP binds with high affinity to its 22 base-pair (bp) DNA recognition site causing a bend of approximately 80–90°.[17] The cage design was based on a DNA tetrahedron[8b] that self-assembles rapidly in high yield in a single annealing step. The cage comprises four oligonucleotides; each DNA strand runs around one face forming double-stranded edges by hybridizing with complementary sequences on the other strands. Five edges are 20 bp long; the sixth, 30 bp, contains the consensus binding site for CAP[17c] (Figure 1).

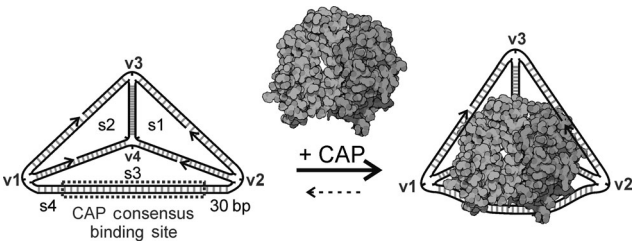


***Figure 1.*** Protein-encapsulating DNA cage designed for the encapsulation of catabolite activator protein (CAP). The cage is made of four oligonucleotides (strands s1–s4). Left: v1–v4 denote vertices 1–4. Right: CAP induces a bend on the binding edge of the DNA cage decreasing the distance between v1 and v2. Illustration of CAP from 1CGP,[17b] representation prepared by D. Goodsell.

The orientation of the CAP-binding site relative to the cage was crucial for encapsulation. It was previously demonstrated that a DNA tetrahedron with 20 bp edges assembles as a single diastereomer, with the major groove facing inwards at the vertices.[8b] As our design is similar, with one edge extended by a full helical turn, the major grooves are also

[*] Dr. C. M. Erben, Dr. J. Periz, Prof. A. J. Turberfield, Dr. A. N. Kapanidis
Biological Physics Research Group, Department of Physics, University of Oxford, Clarendon Laboratory
Parks Road, Oxford, OX1 3PU (UK)
E-mail: a.kapanidis1@physics.ox.ac.uk
Dr. L. M. Hall, Prof. T. Brown
School of Chemistry, University of Southampton
Highfield, Southampton SO17 1BJ (UK)

[**] We thank Dr. Louise Aigrain for helpful discussions. R.C. was supported by the Life Sciences Interface Doctoral Training Centre and Linacre College, University of Oxford. A.N.K. was supported by a European Commission Seventh Framework Program grant (FP7/2007-2013 HEALTH-F4-2008-201418), a UK BBSRC grant (BB/H01795X/1), and a European Research Council grant (261227). L.M.H. was funded by a UK BBSRC Ph.D. studentship. A.J.T. was supported by UK EPSRC grant EP/G037930/1 and a Royal Society-Wolfson Research Merit Award.

Supporting information for this article is available on the WWW under http://dx.doi.org/10.1002/anie.201207914.

expected to face inwards at the vertices. Using the crystal structure of CAP bound to a 30 bp fragment,[17b] we positioned the CAP-binding site such that CAP bound facing into the cage. As a control, we formed a cage with an outward-facing site by shifting the CAP-binding site half a helical turn (5 bp) towards vertex 1 (v1, Figure 1).

To study cage formation and CAP–cage interactions, we titrated both cages (inward and outward site) with CAP and studied the resulting protein–DNA complexes using native polyacrylamide gel electrophoresis (PAGE; Figure 2a). Both cages (lanes 2 and 6) form distinct bands with mobilities lower than a 20 bp DNA tetrahedron[8b] (lane 1), as a result of the inclusion of the longer (30 bp) edge. Adding CAP to the inward-site cage causes a mobility shift, attributed to binding and distortion of the cage by CAP (lanes 3–5). In contrast, CAP has low affinity for the outward-site cage, showing incomplete binding even at an approximately sevenfold molar excess of active CAP (lanes 7–9). CAP does not bind to a cage in which the CAP-binding sequence on the 30 bp edge is replaced (Supporting Information, Figure S1).

The observation of stable CAP binding to the fully assembled inward-site cage was initially surprising because molecular modeling shows that CAP cannot enter or be accommodated inside the cage without deforming one of the tetrahedron edges (Figure S2). It has been observed that both the CAP-cAMP complex[19] and DNA nanostructures[20] exhibit considerable conformational flexibility; we propose that CAP binding and encapsulation occurs by means of transient conformational changes in CAP and the cage. The crystal structure of CAP bound to its recognition site also shows significant deformation of the DNA helix.[17b] We propose that when a conformational fluctuation allows CAP to contact the inward-facing CAP-binding site, CAP binding kinks this edge creating space within the cage by decreasing the distance between vertices 1 and 2 and increasing the distance to the opposing edge (Figure 2b, Figure S2).

The greater affinity of CAP for the inward-site cage may be related to the position of the binding site relative to the vertices. With the inward-site cage, the binding site is positioned in the center of the cage edge. For the outward-site cage, the site was shifted to lie next to vertex 1. The distortion of the outward-site edge caused by CAP binding may be more energetically costly when the site is close to a vertex. CAP also binds the inward-site cage in the absence of cAMP, albeit with a weaker affinity (Figure S3); this result likely reflects that in the absence of cAMP, CAP retains some of its conformational flexibility and affinity for its binding site.[21]

To investigate whether CAP bound in the expected orientation within the cage (Figure 2b), we performed single-molecule experiments using alternating-laser excitation (ALEX) spectroscopy.[18,22] ALEX allows virtual sorting of molecules on two-dimensional histograms of apparent FRET efficiency E* (reporting inter-fluorophore proximity) and probe stoichiometry S. To investigate our system using ALEX, the cage was labeled with Cy3 (the FRET donor) on an unhybridized "hinge" base at vertex 3,[8b] and CAP was labeled with Alexa647 (the FRET acceptor; Figure 2b). CAP was labeled sub-stoichiometrically, with one Alexa647 per dimer on average. For the expected CAP binding orientation in the inward-site cage (Figure 2b), the distances between the donor and the two possible acceptor positions on each monomer are approximately 34 Å and 50 Å for the proximal and distal sites, respectively, with corresponding FRET

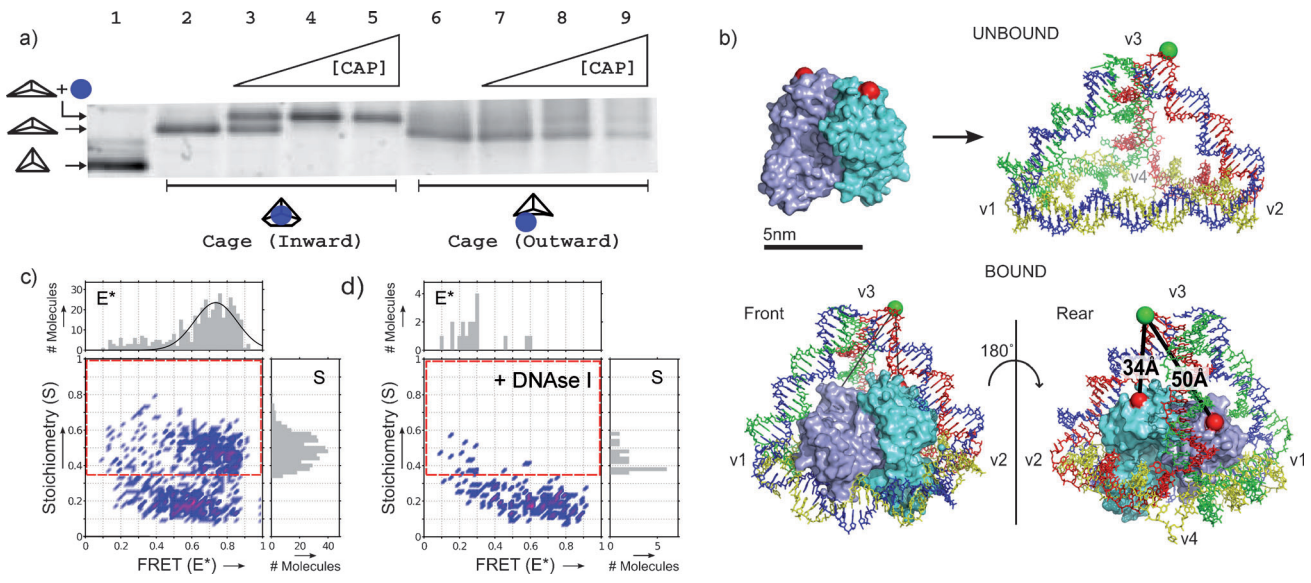


***Figure 2.*** CAP encapsulation within a DNA cage. a) Analysis by native PAGE of inward-site cages (lanes 2–5) and outward-site cages (lanes 6–9) titrated with CAP. Lane 1 contains a 6×20 bp DNA tetrahedron[8b] as a reference. b) Structural model of CAP and the cage in unbound and bound forms (see Experimental Section). Top: Unbound CAP (left, adapted from structure 1CGP)[17b] was labeled sub-stoichiometrically with Alexa647 (red spheres). The unbound cage (right) was labeled at v3 with Cy3 (green sphere). Bottom: cage-encapsulated CAP, front and rear views. Approximate distances between the cage donor (Cy3) and the two CAP acceptors (Alexa647) are shown. c) FRET efficiency (E*) versus stoichiometry (S) histogram[18] of the inward-site cage incubated with CAP. One-dimensional E* and S histograms of the data in the red rectangle are shown at the top and right. d) Same histogram as in (c), after cage digestion by nuclease DNAse I.

efficiencies of approximately 90% and 60%, given the fluorophores used.[23] In contrast, if CAP bound the outside of the cage, the donor–acceptor distance would be greater than 10 nm, with corresponding FRET of less than 5%.

The E*-S histogram for the inward-site cage bound to CAP (Figure 2c) shows two populations: free CAP molecules (acceptor-only molecules characterized by low S values) and CAP–cage complexes (donor–acceptor complexes characterized by intermediate S values and high E* values). The latter complexes comprise a broad population with a mean E* $\approx$ 75%. The high FRET exhibited by this population confirms that CAP is positioned inside the cage. The broad distribution reflects the two labeling positions on CAP.

To test whether CAP can be released upon cage degradation, we incubated the labeled CAP–cage complexes with DNA nuclease I (NEB; see Experimental Section). As expected, the nuclease treatment led to the complete loss of the high-FRET, donor–acceptor population (Figure 2d) while retaining only the free CAP, acceptor-only population, consistent with release of CAP from the cage.

The rate of dissociation of CAP from its DNA site is expected to be reduced by encapsulation, because transient unbinding from DNA is likely to be followed by immediate rebinding to its site: this is a consequence of the high local CAP concentration inside the cage and the favorable positioning of the DNA-binding domains relative to the DNA site. To test the effect of caging on CAP dissociation, we removed cAMP from bound CAP complexes and analyzed the complexes using PAGE (Figure S4). Whilst removal of cAMP clearly causes dissociation of CAP from linear DNA, no apparent dissociation of CAP from the cage was observed on the same timescale.

To quantify this effect of encapsulation on the dissociation kinetics of CAP from the cage, we used ensemble FRET measurements. We first formed CAP–cage complexes (1:1 active CAP/cage) and then added a 50-fold excess of unlabeled competitor DNA with the same binding site as the cage. Upon CAP dissociation from the cage, the donor (on the cage) fluorescence increases: we were thus able to infer the cage-bound fraction of CAP as a function of time (Figure 3, circles; see Experimental Section). The data fit well to a double-exponential decay (dashed line) with a fast component (approximately 60% weighting) with a lifetime of $\tau_1 \approx 41$ s and a much slower component (approximately 40% weighting) with a lifetime of $\tau_2 \approx 3200$ s. The nature of the fast-dissociating CAP–cage complexes is unclear; there may be a subpopulation of cages partially encapsulating CAP. CAP–cage complexes may convert to such an unstable intermediate before dissociation, as suggested in previous work.[22] CAP dissociates much more quickly from linear DNA fragments carrying the same binding site (Figure 3, crosses); the lifetime of this complex $\tau \approx 65$ s is similar to the fast component of the CAP–cage complex. A slight deviation of the data from the single-exponential fit may reflect measurement artifacts (e.g., photobleaching, surface adsorption) or a true subpopulation of more slowly-dissociating complexes.[22] These experiments show that the DNA cage significantly slows CAP dissociation from its binding site.

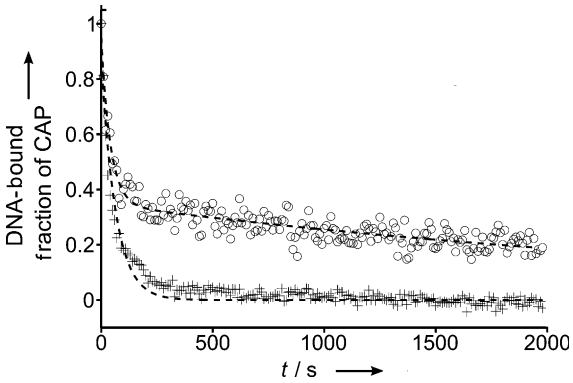


***Figure 3.*** Kinetics of CAP dissociation from a donor-labeled cage (circles) or linear DNA (crosses) using ensemble FRET-quenched donor fluorescence. CAP–DNA complexes were formed at a 1:1 ratio before adding a 50× excess of unlabeled competitor strand at $t = 0$. Plotted is the change in the DNA-bound fraction of CAP (see Experimental Section). Dissociation of CAP from the cage is fitted with a double-exponential decay, resulting in a fast (60% amplitude) and a slow (40% amplitude) component with lifetimes of $\tau_1 = 41 \pm 7$ s and $\tau_2 = 3200 \pm 400$ s, respectively. CAP dissociation from the linear site is fitted with a single-exponential decay with a lifetime of $\tau = 65 \pm 5$ s.

In conclusion, our results demonstrate the non-covalent encapsulation and entrapment of a DNA-binding protein inside a self-assembled DNA cage. Single-molecule FRET measurements on DNA-caged CAP provide distance constraints reporting on the orientation of the protein inside the cage. This technique may be extended to detailed structural studies of caged proteins. Cages can carry several fluorophores as reference points, allowing triangulation of multiple protein–DNA distances using multi-color[24] or switchable FRET;[25] such constraints could be used to ascertain protein structure and conformational dynamics and to study the effects of caging on these properties.

Our results also pave the way for encapsulation of other DNA-binding proteins within DNA cages.[12] Similar approaches can be applied to a wide variety of DNA cages including those based on DNA origami,[26] which could accommodate thousands of proteins. Caging, combined with techniques for triggering conformational changes of the cage,[9d,10] may lead to controllable protein release systems in vivo.

## *Experimental Section*

Oligonucleotides used were ordered from Integrated DNA Technologies, IBA, and ATDBio. Sequences used:

s1: 5′-AGG CAG TTG AGA CGA ACA TTC CTA AGT CTG AAA TTT ATC ACC CGC CAT AGT AGA CGT ATC ACC-3′

s1 iCy3: 5′-AGG CAG TTG AG iCy3 CGA ACA TTC CTA AGT CTG AAA TTT ATC ACC CGC CAT AGT AGA CGT ATC ACC-3′

s2: 5′-CTT GCT ACA CGA TTC AGA CTT AGG AAT GTT CGA CAT GCG AGG GTC CAA TAC CGA CGA TTA CAG-3′

s2 Btn: 5′-CTT GCT ACA CG BTN TTC AGA CTT AGG AAT GTT CGA CAT GCG AGG GTC CAA TAC CGA CGA TTA CAG-3′

s3 CAP Inward: 5′-Phos GGT GAT AAA ACG TGT AGC AAG CTG TAA TCG ACA ATA AAT GTG ATC TAG ATC ACA TTT TAG GAC TAC TAT GGC G-3′

  

s3 CAP Outward: 5′-Phos GGT GAT AAA ACG TGT AGC AAG CTG TAA TCG AAA TGT GAT CTA GAT CAC ATT TTA GGC AAT AAC TAC TAT GGC G-3′

s4 CAP Inward: 5′-Phos CCT CGC ATG ACT CAA CTG CCT GGT GAT ACG ACC TAA AAT GTG ATC TAG ATC ACA TTT ATT GAC GGT ATT GGA C-3′

s4 CAP Outward: 5′-Phos CCT CGC ATG ACT CAA CTG CCT GGT GAT ACG ATA TTG CCT AAA ATG TGA TCT AGA TCA CAT TAC GGT ATT GGA C-3′

s3 Dummy site: 5′-GGT GAT AAA ACG TGT AGC AAG CTG TAA TCG AGT GGA ATT GTG AGC GGA TAA CAA TTT CAC AAC TAC TAT GGC G

s4 Dummy site: 5′-CCT CGC ATG ACT CAA CTG CCT GGT GAT ACG ATG TGA AAT TGT TAT CCG CTC ACA ATT CCA CAC GGT ATT GGA C

ICAP32 TH Top: 5′-C6Amine AC AAT AAA TGT GAT CTA GAT CAC ATT TTA GGA

ICAP32 TH Bot: 5′-TCC TAA AAT GTG ATC TAG ATC ACA TTT ATT GT

Labeling at the 5′-amino-C6-modifying group of ICAP32 TH Top was performed using an *N*-hydroxysuccinimidyl ester of Cy3B (GE Healthcare, Uppsala, Sweden) following the manufacturer's instructions, and was then purified by PAGE.

The structural model shown in Figure 2b was based on a combination of protein structure 1CGP[17b] (CAP bound to a 30 bp dsDNA fragment) and B-DNA strands (20 and 30 bp) formed using molecular modeling software (Ascalaph Designer). The unbound cage contains B-DNA edges only; in the bound cage, the 30 bp edge was replaced manually by that contained in the protein structure. Structures and images were made using MacPyMOL.

To form the DNA cages, equimolar amounts of the four component strands (s1, s2, s3CAP, and s4CAP) were mixed in annealing buffer (20 mM Tris-Cl pH 8.0, 1 mM EDTA, and 500 mM NaCl) to a final concentration of 1 μM, heated to 90 °C for 3 min before cooling to 4 °C over approximately 30 s. DNA cages were purified by PAGE for the single-molecule experiments. To form the linear CAP binding site, ICAP32 TH Top and Bot were annealed in annealing buffer by heating to 94 °C and subsequent cooling to 4 °C over 2 h in steps of 1 °C.

CAP was mutated and labeled with Alexa647 following the method described in [17a]. Labeling efficiency was greater than 90%, measured using a Nanodrop 1000 spectrophotometer. Unlabeled CAP binding activity was approximately 33%, and labeled CAP approximately 20% measured using electrophoretic mobility shift assay (EMSA). "Active" CAP concentrations quoted in the text refer to the concentration of active binding molecules, that is, the percent activity multiplied by the nominal concentration.

For PAGE experiments, CAP–cage complexes were formed using 200 nM cage and a 0×, 0.3×, 3.3×, and 6.7× excess of CAP (Figure 2a, lanes 2–5 and lanes 6–9) at 14 °C for 10 min in KG7 buffer (20 mM HEPES-NaOH pH 7.0, 100 mM potassium-L-glutamate, 10 mM $MgCl_2$, 1 mM DTT, 100 μg mL$^{-1}$ BSA, 1 mM MEA, 5% glycerol) supplemented with 0.2 mM cAMP. Gel conditions were 7.5% 19:1 acrylamide, in Tris-HCl (pH 8.8) with a 4% Tris-HCl (pH 6.8) stacker. Gels were stained with 1× SYBR Gold (Invitrogen) according the manufacturer's instructions before being scanned in a BioRad PharosFX gel scanner.

For single-molecule experiments, CAP–cage complexes were formed using 2 nM PAGE-purified cage with a 1:1 ratio of Alexa647 labeled CAP at RT for 40 min in KG7 buffer and 0.2 mM cAMP (as above). Complexes were then diluted to approximately 50 pM in the presence of 0.2 mM cAMP in KG7 buffer and added to a gasket on a coverslip. The incubated mixture was then examined using single-molecule confocal microscopy as described in [27]. Single-molecule fluorescence bursts were recorded and filtered for those containing red bursts. Data analysis was performed using MATLAB.

To release CAP by digestion of the cage (Figure 2d), 1 unit of DNAse I (NEB, M0303S) was incubated with the same preparation of CAP–cage complexes as for the single-molecule experiments (above) for 30 min at 37 °C in 1× DNAse I reaction buffer before dilution and single-molecule observation.

For ensemble dissociation experiments, CAP–DNA (either cage or linear site) complexes were formed by incubating 10 nM DNA and 10 nM Alexa647-labeled CAP at RT for 5 min in KG7 buffer and 0.2 mM cAMP (as above). A 50× excess of unlabeled ICAP32 competitor DNA was then added, and the increase in donor fluorescence was observed over time. Fluorescence spectra were recorded every 10 s using a Cary Eclipse fluorescence spectrophotometer. The DNA-bound fraction of CAP at time $t$ (Figure 3) was calculated as $(G_{max}-G(t))/(G_{max}-G_{min})$, where $G$ denotes the peak green (donor) fluorescence intensity. $G_{max}$ is the fluorescence intensity from DNA alone, before formation of the complex with red-labeled CAP, multiplied by a dilution factor. $G(t)$ are the measured fluorescence intensities at each timepoint during dissociation and $G_{min}$ is the minimum fluorescence intensity after formation of the initial complex before the addition of the unlabeled competitor DNA.

Received: October 1, 2012
Revised: November 27, 2012
Published online: January 16, 2013

**Keywords:** DNA nanotechnology · drug delivery · protein encapsulation · single-molecule studies · transcription factors

[1] D. Kim, et al., *Stem Cell* **2009**, *4*, 472–476.
[2] C. Sheridan, *Nat. Biotechnol.* **2011**, *29*, 121–128.
[3] a) F. Weiss, J. Elkind, S. C. O'Brien, R. F. Curl, R. E. Smalley, *J. Am. Chem. Soc.* **1988**, *110*, 4464–4465; b) J. Heath, S. O'Brien, Q. Zhang, Y. Liu, R. F. Curl, F. K. Tittel, R. E. Smalley, *J. Am. Chem. Soc.* **1985**, *107*, 7779–7780.
[4] R. Kumar, A. Maitra, P. K. Patanjali, P. Sharma, *Biomaterials* **2005**, *26*, 6743–6753.
[5] V. P. Torchilin, *Nat. Rev. Drug Discovery* **2005**, *4*, 145–160.
[6] Y. Ishitsuka, B. Okumus, S. Arslan, K. H. Chen, T. Ha, *Anal. Chem.* **2010**, *82*, 9694–9701.
[7] Y. Liu, H. Wang, K. Kamei, M. Yan, K.-J. Chen, Q. Yuan, L. Shi, Y. Lu, H.-R. Tseng, *Angew. Chem.* **2011**, *123*, 3114–3118; *Angew. Chem. Int. Ed.* **2011**, *50*, 3058–3062.
[8] a) D. Bhatia, S. Surana, S. Chakraborty, S. P. Koushika, Y. Krishnan, *Nat. Commun.* **2011**, *2*, 339–338; b) R. P. Goodman, I. A. T. Schaap, C. F. Tardin, C. M. Erben, R. M. Berry, C. F. Schmidt, A. J. Turberfield, *Science* **2005**, *310*, 1661–1665.
[9] a) D. Han, S. Pal, J. Nangreave, Z. Deng, Y. Liu, H. Yan, *Science* **2011**, *332*, 342–346; b) S. Douglas, H. Dietz, T. Liedl, B. Högberg, F. Graf, *Nature* **2009**, *459*, 414–418; c) H. Dietz, S. Douglas, W. Shih, *Science* **2009**, *325*, 725–730; d) E. S. Andersen, et al., *Nature* **2009**, *459*, 73–76.
[10] R. Goodman, M. Heilemann, S. Doose, *Nat. Nanotechnol.* **2008**, *3*, 93–96.
[11] a) K. Lu, Q. Duan, L. Ma, D.-X. Zhao, *Bioconjugate Chem.* **2010**, *21*, 187–202; b) M. A. Barry, W. J. Dower, S. A. Johnston, *Nat. Med.* **1996**, *2*, 299–305.
[12] C. M. Erben, R. P. Goodman, A. J. Turberfield, *Angew. Chem.* **2006**, *118*, 7574–7577; *Angew. Chem. Int. Ed.* **2006**, *45*, 7414–7417.
[13] a) H. Lee, et al., *Nat. Nanotechnol.* **2012**, *7*, 389–393; b) A. S. Walsh, H. Yin, C. M. Erben, M. J. A. Wood, A. J. Turberfield, *ACS Nano* **2011**, *5*, 5427–5432.
[14] J. Keuma, H. Bermudez, *Chem. Commun.* **2009**, 7036–7038.
[15] C. Lin, S. Rinker, X. Wang, Y. Liu, N. C. Seeman, H. Yan, *Proc. Natl. Acad. Sci. USA* **2008**, *105*, 17626–17631.
[16] S. Busby, R. Ebright, *J. Mol. Biol.* **1999**, *293*, 199–213.

  

[17] a) A. N. Kapanidis, Y. W. Ebright, R. D. Ludescher, S. Chan, R. H. Ebright, *J. Mol. Biol.* **2001**, *312*, 453 – 468; b) S. C. Schultz, G. C. Shields, T. A. Steitz, *Science* **1991**, *253*, 1001 – 1007; c) R. H. Ebright, Y. W. Ebright, A. Gunasekera, *Nucleic Acids Res.* **1989**, *17*, 10295 – 10305.

[18] A. N. Kapanidis, T. Laurence, N. K. Lee, E. Margeat, X. Kong, S. Weiss, *Acc. Chem. Res.* **2005**, *38*, 523 – 533.

[19] a) S. R. Tzeng, C. G. Kalodimos, *Nature* **2012**, *488*, 236 – 240; b) P. Kumar, D. C. Joshi, M. Akif, Y. Akhter, S. E. Hasnain, S. C. Mande, *Biophys. J.* **2010**, *98*, 305 – 314.

[20] B. K. Müller, A. Reuter, F. C. Simmel, D. C. Lamb, *Nano Lett.* **2006**, *6*, 2814 – 2820.

[21] T. Heyduk, J. C. Lee, *Proc. Natl. Acad. Sci. USA* **1990**, *87*, 1744 – 1748.

[22] A. N. Kapanidis, N. K. Lee, T. A. Laurence, S. Doose, E. Margeat, S. Weiss, *Proc. Natl. Acad. Sci. USA* **2004**, *101*, 8936 – 8941.

[23] R. Crawford, D. J. Kelly, A. N. Kapanidis, *ChemPhysChem* **2012**, *13*, 918 – 922.

[24] J. Lee, S. Lee, K. Ragunathan, C. Joo, T. Ha, S. Hohng, *Angew. Chem.* **2010**, *122*, 10118 – 10121; *Angew. Chem. Int. Ed.* **2010**, *49*, 9922 – 9925.

[25] S. Uphoff, S. J. Holden, L. L. Reste, J. Periz, S. v. d. Linde, M. Heilemann, A. N. Kapanidis, *Nat. Methods* **2010**, *7*, 831 – 836.

[26] Y. Ke, J. Sharma, M. Liu, K. Jahn, Y. Liu, H. Yan, *Nano Lett.* **2009**, *9*, 2445 – 2447.

[27] K. Lymperopoulos, R. Crawford, J. Torella, M. Heilemann, L. C. Hwang, S. J. Holden, A. N. Kapanidis, *Angew. Chem.* **2010**, *122*, 1338 – 1342; *Angew. Chem. Int. Ed.* **2010**, *49*, 1316 – 1320.

  